ACS OMEGA

Open Access

http://pubs.acs.org/journal/acsodf

Article

Cell Penetrability of a γ-Crystallin Peptide Fragment from the Discarded Cataractous Eye Emulsion

Prasun Chowdhury, Atul Kumar Ojha, Shishir Bhowmik, Krishna Halder, Kabira Sabnam, Sujan Santra, Koel Chaudhury, and Swagata Dasgupta*

Cite This: *ACS Omega* 2024, 9, 14840−14848

Read Online

ACCESS | Metrics & More | Article Recommendations | Supporting Information

ABSTRACT: The efficiency of the intracellular transport of medication and target specificity is frequently hampered by biological obstacles. The potential for therapeutic use of peptide fragments from naturally occurring proteins is promising, as peptides exhibit high selectivity due to several possibilities of interaction with their target. Certain peptide sequences, often referred to as cell-penetrating peptides (CPPs), are those that can penetrate cell membranes. Our goal is to find these sequences in the discarded postcataractery surgery emulsion known as the cataractous eye protein isolate (CEPI). One peptide fragment from this discarded protein has been identified to be a potential CPP based on the similarities with other well-known CPPs. Cell membrane penetrability and cytotoxicity of the peptide have been investigated. Fibroblast cells were incubated with the fluorescently labeled peptide and were observed under fluorescence as well as under confocal microscopy. It was found that the peptide possesses a cell-penetrating ability.

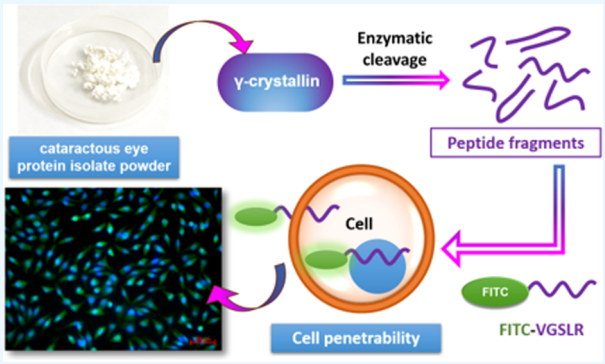

1. INTRODUCTION

There has been an exponential increase in the development and use of peptide drugs in the last couple of decades. While it has been recognized that peptides could be advantageous primarily because of their selectivity and low toxicity, plasma stability and oral bioavailability pose a problem. The advancement in their chemical, structural, and mechanistic aspects has thus led to the development of peptide drugs.[1] Small-molecule drugs often face the challenge of target specificity and cell membrane permeability. Biological barriers, such as cell membranes, often restrict intercellular drug delivery options that, in turn, affect the target specificity. This hampers systemic drug distribution and limits the therapeutic value. It is possible to enhance both the therapeutic value and on-target specificity of nonpermeable drugs with compounds that can effectively penetrate the cell membrane. In this regard, peptides are a good option because the specific properties they possess can be exploited to elicit selectivity in target selection and the mode of action. These peptide fragments from naturally occurring proteins have been found to have therapeutic applications.[2] Additionally, there are particular peptide sequences that can penetrate through cell membranes. These peptides find applications in therapeutics for transporting a wide variety of biologically active molecules across the cell membrane. Peptide sequences commonly known as cell-penetrating peptides (CPPs) from different proteins have been identified. Some of the examples of such sequences are given in Table 1.

Table 1. Peptide Sequence of CPPs from Different Proteins

sequence	protein of occurrence
GRKKRRQRRRPPQ[3]	HIV-1 TAT
RKKRRQRRR[4]	HIV-1 TAT
RQIKIWFQNRRMKWKK[5]	antennapedia homeodomain
KETWWETWWTEWSQPKKKRKV[6]	T antigen NLS
MVKSKIGSWILVLFVAMWSDVGLCKKRP[7]	bovine prion protein

CPPs have also gained attention in anticancer research as a drug delivery factor.[8,9] Moreover, for many physiological processes, peptides act as intrinsic signaling molecules, granting them an advantage to be used as a therapeutic intervention for mimicking natural pathways. In addition, studies have shown that short fragments of peptides from natural sources have anticoagulation effects. A novel

Received: October 3, 2023
Revised: January 25, 2024
Accepted: February 13, 2024
Published: March 6, 2024

antithrombotic peptide sequence YQEPVLGPVR obtained from β-casein having antithrombotic activity is one such example.[10] Recent studies have explored the cell penetration ability of peptide sequences derived from milk proteins (bovine α-S1-casein).[11] Specific CPPs explicitly target cancer cells or tumor cells and find application as anticancer peptides or tumor-homing peptides, respectively.[12] A peptide sequence (p28) from azurin (sequence 50−77) has been shown to penetrate breast cancer cells preferentially and induce apoptosis.[13] This peptide p28 (NSC745104) is currently in phase I clinical trials.[14] Furthermore, p28 was observed to cross the blood−brain barrier, localize especially to tumor lesions, and enhance the effectiveness of DNA-damaging agents.[15] Guidotti et al. have listed several CPPs that are under preclinical and clinical trials.[16]

The human eye lens is abundant in water-soluble proteins called crystallins[17] that are broadly classified as α-, β-, and γ-crystallins.[18,19] The transparency of the lens is preserved by crystallins, which have a high refractive index. Proteins aggregate or cross-link as a result of a variety of factors, including aging, mutations, protein oxidation, etc. This can cause cataract, an opacification of the eye lens that can cause permanent blindness.[20] Cataract surgery, which involves removing the opaque lens and replacing it with a durable artificial intraocular lens, has been the only available treatment for cataracts to date.[21] The total annual number of cataract operations carried out in India increased from 1.2 million in the 1980s to 6.4 million by the year 2020.[22,23] After surgery, the proteins can be extracted from cataractous lens emulsions, which are otherwise discarded. The cataractous eye protein isolate (CEPI) is the name given to this protein.[24]

The CEPI obtained from a discarded source has been used for fragmentation to check any possible similarity with other peptide fragments of use following which the cell membrane permeability of the obtained fragments has been monitored.

2. EXPERIMENTAL SECTION

2.1. Materials. The Sathi Eye Clinic in Kharagpur, India, provided the protein emulsion that was produced following phacoemulsification surgery (approved by the Institute Ethical Committee Approval Letter, Indian Institute of Technology Kharagpur, West Bengal, India, letter No IIT/SRIC/DR/2018). The custom peptide VGSLR and fluorescein isothiocyanate tagged peptide (FITC-VGSLR) were purchased from SBioChem, Thrissur, Kerala, India. Cellulose membrane (MWCO = 12.6 kDa) was purchased from Sigma Chemical Co. All other chemicals used, unless specified, were purchased from SRL, India, and were of analytical grade.

2.2. Methods. *2.2.1. Purification of CEPI.* The emulsion produced following cataract surgery was obtained in an autoclaved vessel and stored at 4 °C until further use. An earlier approach from this laboratory was used to isolate and purify the protein.[25−27] In brief, the emulsion was centrifuged at 4 °C and 7900 rpm for 40 min. The supernatant was collected and lyophilized. The dried sample was then dissolved in double-distilled water, dialyzed with a cellulose membrane (MWCO 12.6 kDa) for 48 h in 10 mM phosphate buffer (pH 7.4), and then dialyzed again in double-distilled water for a further 48 h. The dialyzed emulsion was lyophilized, and the resulting dry mass was kept at 0 °C until use.

2.2.2. Theoretical Trypsin Digestion, Hydropathicity, and pI Calculation. Trypsin digestion to know the sequence and mass of the fragments obtained from the polypeptide sequence was performed on the web portal Expasy: peptide mass (https://web.expasy.org/peptide_mass/).[28] The one-letter amino acid sequence of the protein, obtained from the RCSB PDB (https://www.rcsb.org/) (PDB IDs: 1HK0, 2JDF, 2NBR), was entered, and trypsin was selected as the enzyme and iodoacetamide was selected to treat cysteines to form carbamidomethyl-cysteine (Cys_CAM).

Grand average of hydropathicity (GRAVY) score and the *pI* of the obtained fragments were calculated using the ProtParam tool of Expasy (https://web.expasy.org/protparam/).[28] ProtParam is a tool that enables the computation of numerous physical and chemical parameters for a given peptide sequence.

2.2.3. Trypsin Digestion. Trypsin digestion of the treated CEPI was performed to cleave the protein into small peptide fragments. The in-solution protein digestion protocol was adopted from Promega (Sequencing grade Modified Trypsin Certificate of Analysis 9PIV511). CEPI protein was dissolved in 50 mM ammonium bicarbonate in water. To this, 45 mM dithiothreitol (DTT) in 50 mM ammonium bicarbonate solution was added to reduce the disulfide bonds and incubated for 15 min at 50 C. For the alkylation of cystines, 100 mM iodoacetamide (IAA) in 50 mM ammonium bicarbonate solution was added. This solution was incubated at room temperature for 15 min in the dark. Unreacted IAA in the mixture was treated with 1 μL of previously used DTT. This was mixed with a small volume aliquot of trypsin stock solution to make the ratio of the enzyme: substrates 1:50 (mass:mass). The solution was incubated overnight at 37 C. After the incubation, the enzyme activity was quenched by the addition of a highly concentrated (i.e., 10%) trifluoroacetic acid (TFA).

2.2.4. Matrix-Assisted Laser Desorption Ionization Spectroscopy-Time-of-Flight (MALDI ToF). MALDI experiments were performed on a Bruker Daltonics Ultraflex MALDI ToF/ToF mass spectrometer (Germany). The matrix was prepared by dissolving 20 mg/mL of sinapinic acid (3,5-dimethoxy-4-hydroxycinnamic acid) in 1:1 v/v water and HPLC-grade acetonitrile containing 1% TFA just before the experiments. The trypsin-digested protein solution was then mixed with the matrix solution in a 1:1 ratio for measurements. The sample was then spotted on a steel plate and left for 30 min to dry. Scanning was done using an accelerating voltage of 20 kV, and positive ions were collected in the detector by using a reflection method. A linear acquisition mode with 3500 laser shots and a mass range over an m/z range from 5 to 50 kDa were employed for the detection.

2.2.5. Cell Proliferation Assay. The cell proliferative properties of the conjugated peptide (FITC-VGSLR) and unconjugated peptide (VGSLR) on L929 cells were measured by using the MTT test. Cells were seeded at a density of 0.5×10^4 cells per well in 96-well plates and then incubated with 100 μL of complete media for 24 h before being treated with peptides at various concentrations (10, 25, 50, and 100 μM). After 48 h, the cells were incubated with MTT at 37 °C for 4 h in the dark, and then, 100 μL of dimethyl sulfoxide (DMSO) was added to remove the purple formazan crystals. The absorbance at 570 nm was recorded, and the % cell viability was determined by calculating the ratio of treated cell absorbance to untreated cell absorbance

$$\%\ \text{cell viability} = \frac{OD_{570}[\text{sample}] - OD_{570}[\text{blank}]}{OD_{570}[\text{control}] - OD_{570}[\text{blank}]} \times 100$$

https://doi.org/10.1021/acsomega.3c07665
ACS Omega 2024, 9, 14840−14848

Table 2. Peptide Sequences and Their Masses Obtained after Trypsin Digestion of γD Crystallin with ExPasy

peptide sequence	position	modification	mass
FNEIHSLNVLEGSWVLYELSNYR	117−139		2782.3835
VDSGCWMLYEQPNYSGLQYFLR	37−58	Cys_CAM: 41	2669.2163/2726.2377
HYECSSDHPNLQPYLSR	15−31	Cys_CAM: 18	2045.9134/2102.9348
GDYADHQQWMGLSDSVR	60−76		1964.8555
GQMIEFTEDCSCLQDR	99−114	Cys_CAM: 108, 110	1874.7717/1988.8146
QYLLMPGDYR	142−151		1255.6139
YQDWGATNAR	153−162		1181.5334
LIPHSGSHR	80−88		1003.5432
ITLYEDR	3−9		909.4676
EDYR	95−98		582.2518
LYER	91−94		580.3089
VIDFS	169−173		580.2977
GFQGR	10−14		564.2888
CNSAR	32−36	Cys_CAM: 32	550.2402/607.2617
VGSLR	**163−167**		**531.3249**

Table 3. Theoretical pI and GRAVY Scores of Peptide Fragments of γD Crystallin

γD crystallin				
peptide sequence	no. of AA	mol. wt.	theoretical *pI*	GRAVY score
FNEIHSLNVLEGSWVLYELSNYR	23	2783.09	4.75	−0.178
VDSGCWMLYEQPNYSGLQYFLR	22	2670.01	4.37	−0.364
HYECSSDHPNLQPYLSR	17	2046.20	5.99	−1.353
GDYADHQQWMGLSDSVR	17	1965.08	4.41	−1.065
GQMIEFTEDCSCLQDR	16	1875.07	3.92	−0.588
QYLLMPGDYR	10	1255.45	5.83	−0.660
YQDWGATNAR	10	1181.23	5.84	−1.470
LIPHSGSHR	9	1003.13	9.76	−0.689
ITLYEDR	7	909.01	4.37	−0.743
EDYR	4			
LYER	4			
VIDFS	5	579.65	3.80	1.440
GFQGR	5	563.61	9.75	−1.200
CNSAR	5	549.60	8.25	−0.900
VGSLR	5	530.62	9.72	0.460

Table 4. Theoretical *pI* and GRAVY Scores of Known CPPs

peptide	sequence	mol. wt.	theoretical *pI*	GRAVY score
	Hydrophobic CPPs			
Bip4	VSALK[35]	516.64	8.72	1.020
C105Y	CSIPPEVKFNPFVYLI[36]	1866.25	5.99	0.719
melittin	GIGAVLKVLTTGLPALISWKRKRQQ[37]	2734.33	12.02	0.104
gH625	HGLASTLTRWAHYNALIRAF[38]	2298.64	10.84	0.110
	Cationic CPPs			
TAT	RKKRRQRRR[39]	1339.62	12.70	−4.256
R8	RRRRRRRR[40]	1267.52	12.85	−4.500
DPV3	RKKRRRESRKKRRRES[41]	2212.60	12.23	−3.763
DPV6	GRPRESGKKRKRKRLKP[41]	2077.51	12.19	−2.735
penetratin	RQIKIWFQNRRMKWKK[42]	2246.75	12.31	−1.731
R9-TAT	GRRRRRRRRRPPQ[43]	1803.12	12.90	−3.662
	Amphipathic CPPs			
pVEC	LLIILRRRIRKQAHAHSK[44]	2209.72	12.48	−0.444
ARF (19−31)	RVRVFVVHIPRLT[45]	1591.97	12.30	0.685
MPG	GALFLGFLGAAGSTMGAWSQPKKKRKV[46]	2807.35	11.33	−0.004
MAP	KLALKLALKALKAALKLA[47]	1877.47	10.60	0.994
transportan	GWTLNSAGYLLGKINLKALAALAKKIL[48]	2841.48	10.18	0.633

2.2.6. Membrane Penetrability of the Peptide. The ability of the peptide to penetrate the cell membrane was investigated by incubating fibroblast cells with the fluorescein isothiocyanate tagged peptide (FITC-VGSLR) and visualizing the cells

https://doi.org/10.1021/acsomega.3c07665
ACS Omega 2024, 9, 14840−14848

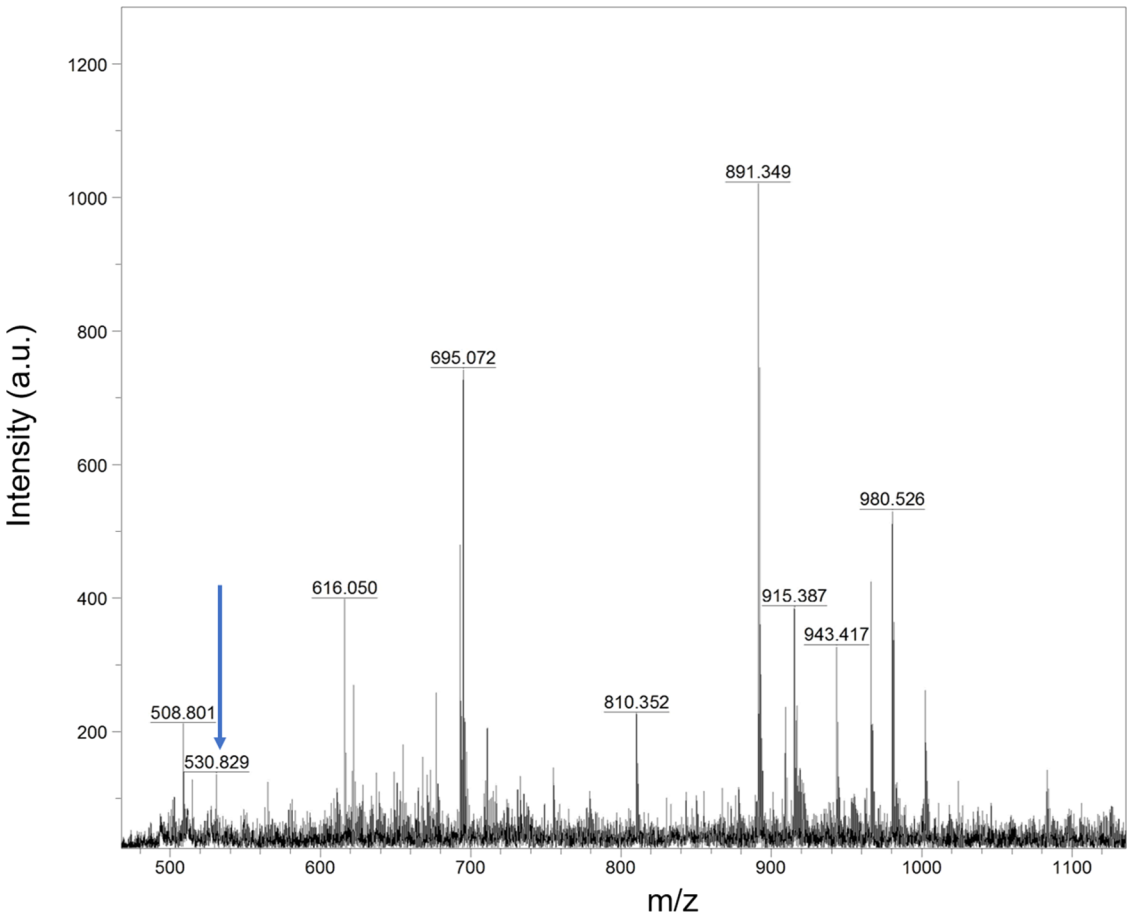

Figure 1. MALDI ToF mass spectra of trypsin-digested CEPI showing the peptide fragment VGSLR (blue arrow).

under fluorescence microscopy as well as under confocal microscopy. 3T3 cells were grown on lysine-coated coverslips and later fixed with 3.7% paraformaldehyde in PBS for 20 min. Cells were washed and incubated with 50 μM of the tagged peptide in PBS for 6 h at 4 °C. The peptide solution was removed, and cells were washed with PBS. Cells were permeabilized with 1% (v/v) Triton-X 100 (Sigma-Aldrich) in PBS for 15 min followed by blocking in 3% BSA. The nuclei were subsequently stained with 4,6-diamidino-2-phenylindole (DAPI; Sigma-Aldrich) for 10 min. Imaging was done using an inverted fluorescence microscope (Axio Observer, Carl Zeiss, Germany) and a confocal microscope (Leica TCS SP8, Leica Microsystems). To check the localization of the peptide in live cells, peptides were incubated following a previously reported method with slight modification.[29] In brief, 3T3 and L929 cells with a density of 0.5×10^4 were cultured and incubated with 50 μM of peptides in growth media. The peptide solution was removed by washing the cells with PBS. DAPI staining of the nuclei was done for 3T3 cells, whereas L929 cells were viewed without DAPI staining. The nonconjugated peptide fragment VGSLR was used as a negative control. Control experiments with FITC-V were performed to ensure localization efficacy.

3. RESULTS AND DISCUSSION

3.1. Theoretical Protein Cleavage. The determination of the possible fragments of the protein following trypsin digestion was undertaken with the help of ExPasy. Trypsin was the selected enzyme, and iodoacetamide was selected to treat cysteines. The α-crystallin and β-crystallin are oligomeric

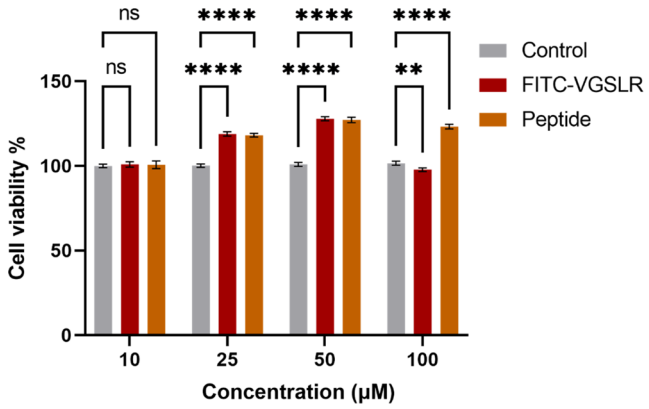

Figure 2. Cell viability studies of L929 on FITC-VGSLR and the unconjugated peptide. MTT assay data presented as mean ± SD; p-values are calculated using a two-way ANOVA test, * = $p < 0.05$, ** = $p < 0.01$, *** = $p < 0.001$, **** = $p < 0.0001$, and n.s. = not significant.

proteins with higher molecular weights (50−800kD), whereas γ-crystallin is a monomeric protein of lower molecular weight (~21kD).[30] Earlier studies show the presence of γ-crystallin in the discarded cataractous emulsion.[31] The difference in molecular weight facilitates the separation of the α-crystallin and β-crystallin from γ-crystallin via centrifugation.[24] Water-soluble γ-crystallin is found to be present in the supernatant post centrifugation.[31] Following a previous procedure from our lab, we have obtained γ-crystallin from the CEPI.[25,31,32] In

https://doi.org/10.1021/acsomega.3c07665
ACS Omega 2024, 9, 14840−14848

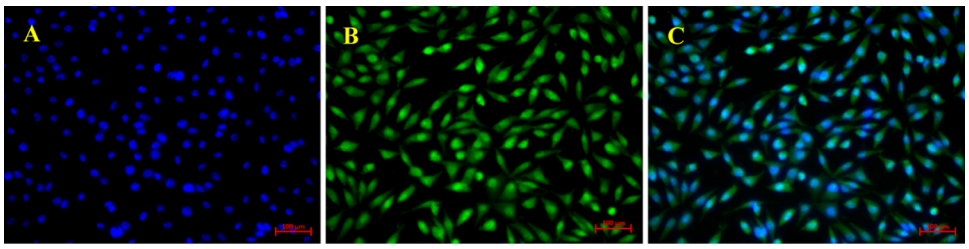

Figure 3. Fluorescence microscopic image of the cell incubated with the labeled peptide (FITC-VGSLR). (A) DAPI-stained nuclei, (B) localization of FITC-VGSLR in the cell, and (C) merged image of DAPI (blue) and FITC-VGSLR (green).

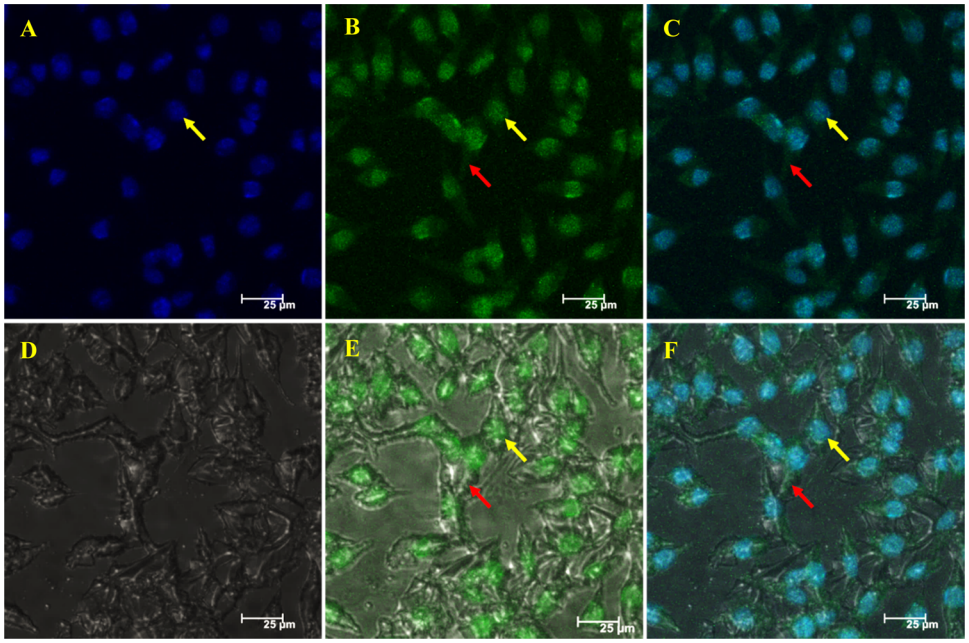

Figure 4. Confocal microscopy images of cells incubated with labeled peptide (FITC-VGSLR). (A) DAPI-stained nuclei, (B) localization of FITC-VGSLR in the cell, (C) merged image of DAPI (blue) and FITC-VGSLR (green), (D) brightfield image (differential interference contrast) showing the cells, (E) fluorescence image of FITC-VGSLR and brightfield image overlaid, and (F) fluorescence image of DAPI, FITC-VGSLR, and brightfield image overlaid. Yellow arrow: nuclei, red arrow: cytoplasm.

addition, theoretical trypsin digestion was performed on the sequence of human γ-crystallin. The result of the cleavage of γD crystallin (PDB ID: 1HK0) is shown in Table 2 (γB and γC crystallin are shown in Tables S1 and S2 of the Supporting Information, respectively).

3.2. Theoretical Calculations. The hydropathy values of all of the amino acids, from Kyte and Doolittle scale, added together and divided by the number of residues in the sequence yield the GRAVY value for a given peptide.[33] A hydrophilic peptide has a low negative GRAVY score, while a hydrophobic peptide has a comparatively high positive GRAVY score. The GRAVY value and *pI* of the obtained fragments were calculated. Calculations were also done for the known cell-penetrating peptides (CPPs). The results are presented in Tables 3 and 4, respectively. It was observed that the sequence VGSLR from γD crystallin has some similarities to a known hydrophobic cell-penetrating peptide Bip4 (VSALK). Table 3 shows the molecular weight, *pI*, and GRAVY score of the peptide VGSLR. Table 4 shows the same for cell-penetrating peptides, including Bip4 (VSALK). The GRAVY score of the fragment VGSLR is 0.460, which is in the range (0.680 to −0.440) of other known amphipathic CPPs. This peptide has one basic amino acid, one polar uncharged amino acid, and no acidic amino acid residue. Moreover, its GRAVY score is within the range of −0.5 ∼ + 0.5; thus, it can be categorized as a cationic amphiphilic peptide.[34]

3.3. MALDI ToF of the CEPI Digested by Trypsin. Trypsin digestion was performed to check the fragmentation of CEPI. MALDI ToF was performed to check the mass of the fragment produced after digestion. The mass spectra are shown in Figure 1. The calculated molecular weight of VGSLR is 530.62, as shown in Table 3. The peak at 530.829 *m*/*z* most likely corresponds to the molecular ion peak of the VGSLR fragment. The observed peak presumably differs from the theoretical value due to deprotonation of the peptide.[49]

3.4. Characterization of the Peptide VGSLR and FITC-VGSLR. As we have seen the similarities in the peptide fragment VGSLR and hydrophobic cell-penetrating peptides Bip4 (VSALK), the peptide VGSLR and fluorescein isothiocyanate tagged peptide (FITC-VGSLR) were purchased following customized synthesis from SBioChem, Thrissur, Kerala, India. The details of the peptides, analytical HPLC trace chromatogram, and mass spectra are provided in the Supporting Information, Figures S1−S4.

3.5. Cytotoxicity of the Peptide. Cytotoxicity of the fluorescent conjugated peptide (FITC-VGSLR) and peptide (VGSLR) was tested by using the standard MTT assay. A range of sample concentrations of the peptide (10, 25, 50, and

https://doi.org/10.1021/acsomega.3c07665
ACS Omega 2024, 9, 14840−14848

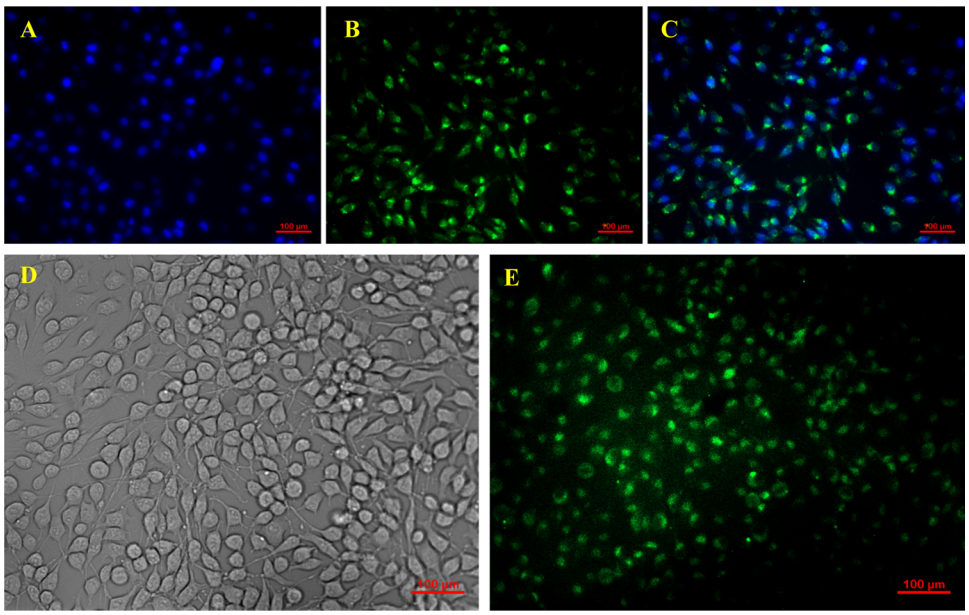

Figure 5. Fluorescence microscopic image of the cell incubated with the labeled peptide (FITC-VGSLR) without fixation on cells 3T3 (A−C) and cell L929 (C−D). (A) DAPI-stained nuclei, (B) localization of FITC-VGSLR in the cell, (C) merged image of DAPI (blue) and FITC-VGSLR (green), (D) brightfield image showing L929 cell, and (E) localization of FITC-VGSLR in the L929 cell.

100 μM) were monitored, and a higher proliferation was observed at (50 μM) with the conjugated peptides compared to the untreated cells ($p < 0.0001$). Figure 2 shows the percentage viability of the L929 cells at different concentrations of the FITC-peptide and unconjugated peptide. The cellular viability increased progressively from 25 and 50 μM compared to 10 μM for both FITC-VGSLR and VGSLR. This suggests that the peptide VGSLR is conducive to cell growth and has a proliferative effect on the cells. Pentapeptide fragments derived from the Ku70 protein homologous to VGSLR were found to have antiapoptotic effects in human, mouse, and rat cells.[50] This could be the probable reason for the observed increase in the proliferation of cells with a higher concentration of peptides. Since the peptide did not show any significant toxicity toward the cells in the range of concentrations tested, IC50 values could not be calculated. FITC-peptide-treated samples showed reduced viability at 100 μM, possibly due to the cytotoxic effects of FITC at higher concentrations.[51]

3.6. Membrane Penetrability and Distribution of the Peptide. To check the cell membrane penetrability and distribution of the peptide, cells incubated with the labeled peptide (FITC-VGSLR) were analyzed under fluorescence microscopy. The image of fluorescence microscopy revealing the subcellular localization of FITC-VGSLR is shown in Figure 3. The DAPI-stained nuclei are shown in Figure 3A. It was observed that the labeled peptide successfully penetrated the cell membrane and was found to be distributed in the cell cytoplasm (Figure 3C). It was also observed that the peptide was able to penetrate the nucleus of the cell (Figure 3B). From the confocal microscopy images (Figure 4), it was observed that the localization of the peptide at the nucleus was more than that in the cytoplasm. The nuclei have been indicated by yellow arrows and the cytoplasm with red arrows. A similar type of localization of CPPs, in both the cytoplasm and nucleus, was shown by D-Tat, R9-Tat, and Tat-(48−60) peptides as reported by Futaki et al.[43] Rhee et al. have reported that the peptide C105Y showed an enriched fluorescence signal in the nucleus in addition to being present in the cytoplasm.[36] The localization of the fluorescent-tagged C105Y peptide was studied under cell fixation conditions on mouse fibroblast 3T3 cells (along with other cell lines), and the reported observations were found to be similar to that of FITC-VGSLR on 3T3 cells. Gomez et al. have shown that a series of pentapeptides (Table S3, Supporting Information) including VSALK based on the Bax-binging domain of Ku70 have good cell-penetrating ability.[35] The reported peptide sequences are homologous to the peptide VGSLR. To confirm that the observed cell penetration of the peptide is not due to the fixation of cells, FITC-VGSLR was incubated with live cells and observed under fluorescence microscopy. Live cells (3T3 and L929) were incubated with an optimized dose treatment of FITC-VGSLR, and the images are shown in Figure 5. After incubation with the labeled peptide, 3T3 cells were fixed and stained with DAPI (Figure 5A). It was observed that the peptide was localized in both the cytoplasm and the nuclei of the cells (Figure 5B). In comparison to our earlier observation on fixed cells, the localization in the cytoplasm was to a greater extent than in the nucleus. It is known that even mild fixation can alter the cellular uptake or redistribution of peptides and generate a false positive result;[52] hence, we have performed live cell imaging of cells L929 without DAPI staining. Intracellular localization for FITC- VGSLR was clearly evident via fluorescence images, suggesting cellular uptake and distribution in the cytoplasm more than the nucleus (Figure 5D). Thus, the enhanced localization within the nucleus that was observed earlier (Figures 3 and 4) could be due to the effect of fixation.[52] In order to confirm that the peptide is responsible for cell penetration rather than FITC, a control experiment utilizing FITC-V (valine-conjugated) was carried out on live cells (L929). There was no discernible FITC-V localization within the cells (Figure S5, Supporting Information), which suggests that the localization of FITC-VGSLR is due to the cell-penetrating ability of the peptide. Negative control experiments were performed on L929 live cells with the unconjugated peptide fragment (VGSLR). It may be noted

https://doi.org/10.1021/acsomega.3c07665
ACS Omega 2024, 9, 14840−14848

that as the peptide does not have any fluorophore, no clear fluorescence signals are observed under fluorescence microscopy apart from some low-intensity signals from the media itself (Figure S6, Supporting Information). To ensure that the cell penetration is due to the peptide and not FITC, control experiments using FITC-V (valine-conjugated) were performed on live cells (L929) (Figure S5 in the Supporting Information).

4. CONCLUSIONS

We processed the discarded cataractous eye lens emulsion to identify specific proteins of interest. Theoretical studies of trypsin digestion of the protein indicated the presence of several fragments with their corresponding mass. Calculation of the *pI* and the GRAVY score of the fragments obtained with those of several known cell-penetrating peptide sequences identified VGSLR as a possible candidate. The cell membrane penetrability of the peptide fragment was monitored with the FITC-labeled peptide (FITC-VGSLR). The tagged peptide fragment was incubated with fibroblast cells and analyzed by fluorescence microscopy. The results showed that the peptide VGSLR possesses the ability to penetrate cell membranes. The cytotoxicity of the labeled peptide was tested, and it was observed that the peptide does not show any toxicity. These studies indicate that the peptide can be proposed as a potential therapeutic unit for drug delivery to carry cargo to cells because of its cell-penetrating abilities and noncytotoxicity properties.

■ ASSOCIATED CONTENT

Supporting Information

The Supporting Information is available free of charge at https://pubs.acs.org/doi/10.1021/acsomega.3c07665.

Peptide sequences and their masses obtained after theoretical trypsin digestion of γB crystallin (PDB ID 2JDF) and γC crystallin (PDB ID 2NBR); sequence of peptides having cell penetrability reported by Gomez et al.; characterization of the peptides VGSLR and FITC-VGSLR; analytical HPLC trace chromatogram of peptides VGSLR and FITC-VGSLR; ESI-MS mass spectra of the peptides VGSLR and FITC-VGSLR; fluorescence microscopic images of the cell incubated with FITC-V; fluorescence microscopic images of the L929 cells incubated with VGSLR as the negative control; characterization of the FITC-V; and MALDI ToF mass spectra of FITC-V (PDF)

■ AUTHOR INFORMATION

Corresponding Author

Swagata Dasgupta − *Department of Chemistry, Indian Institute of Technology Kharagpur, Kharagpur 721302, India;* orcid.org/0000-0003-2074-1247; Phone: +91-3222-283306; Email: swagata@chem.iitkgp.ac.in; Fax: +91-3222-282252

Authors

Prasun Chowdhury − *Department of Chemistry, Indian Institute of Technology Kharagpur, Kharagpur 721302, India;* orcid.org/0009-0003-8612-3772

Atul Kumar Ojha − *School of Medical Science and Technology, Indian Institute of Technology Kharagpur, Kharagpur 721302, India;* orcid.org/0000-0001-7577-8587

Shishir Bhowmik − *Department of Chemistry, Indian Institute of Technology Kharagpur, Kharagpur 721302, India*

Krishna Halder − *Department of Chemistry, Indian Institute of Technology Kharagpur, Kharagpur 721302, India*

Kabira Sabnam − *Department of Chemistry, Indian Institute of Technology Kharagpur, Kharagpur 721302, India*

Sujan Santra − *Department of Chemistry, Indian Institute of Technology Kharagpur, Kharagpur 721302, India*

Koel Chaudhury − *School of Medical Science and Technology, Indian Institute of Technology Kharagpur, Kharagpur 721302, India;* orcid.org/0000-0002-9390-1179

Complete contact information is available at: https://pubs.acs.org/10.1021/acsomega.3c07665

Notes

The authors declare no competing financial interest.

■ ACKNOWLEDGMENTS

The authors are thankful to Central Research Facility, IIT Kharagpur, for providing instrumental facilities. The use of the facilities in the laboratory of Prof. S. DasGupta, Department of Chemical Engineering, IIT Kharagpur are gratefully acknowledged. SERB is acknowledged for the project CRG/2021/004375-G, Dt: 24-11-2021. P.C., A.K.O., K.H., and K.S. thank the Ministry of Education (MoE), Government of India (GoI), for their fellowship, and S.S. thanks "Innovation in Science Pursuit for Inspired Research" (INSPIRE), Ministry of Science and Technology, GoI, for his fellowship.

■ REFERENCES

(1) Muttenthaler, M.; King, G. F.; Adams, D. J.; Alewood, P. F. Trends in Peptide Drug Discovery. *Nat. Rev. Drug Discovery* **2021**, *20* (4), 309−325.

(2) Lau, J. L.; Dunn, M. K. Therapeutic Peptides: Historical Perspectives, Current Development Trends, and Future Directions. *Bioorg. Med. Chem.* **2018**, *26* (10), 2700−2707.

(3) Vivès, E.; Brodin, P.; Lebleu, B. A Truncated HIV-1 Tat Protein Basic Domain Rapidly Translocates through the Plasma Membrane and Accumulates in the Cell Nucleus. *J. Biol. Chem.* **1997**, *272* (25), 16010−16017.

(4) Park, J.; Ryu, J.; Kim, K.-A.; Lee, H. J.; Bahn, J. H.; Han, K.; Choi, E. Y.; Lee, K. S.; Kwon, H. Y.; Choi, S. Y. Mutational Analysis of a Human Immunodeficiency Virus Type 1 Tat Protein Transduction Domain Which Is Required for Delivery of an Exogenous Protein into Mammalian Cells. *J. Gen. Virol.* **2002**, *83* (5), 1173−1181.

(5) Derossi, D.; Joliot, A. H.; Chassaing, G.; Prochiantz, A. The Third Helix of the Antennapedia Homeodomain Translocates through Biological Membranes. *J. Biol. Chem.* **1994**, *269* (14), 10444−10450.

(6) Morris, M. C.; Deshayes, S.; Heitz, F.; Divita, G. Cell-Penetrating Peptides: From Molecular Mechanisms to Therapeutics. *Biol. Cell* **2008**, *100* (4), 201−217.

(7) Magzoub, M.; Sandgren, S.; Lundberg, P.; Oglęcka, K.; Lilja, J.; Wittrup, A.; Göran Eriksson, L. E.; Langel, Ü.; Belting, M.; Gräslund, A. N-Terminal Peptides from Unprocessed Prion Proteins Enter Cells by Macropinocytosis. *Biochem. Biophys. Res. Commun.* **2006**, *348* (2), 379−385.

(8) Klimpel, A.; Lützenburg, T.; Neundorf, I. Recent Advances of Anti-Cancer Therapies Including the Use of Cell-Penetrating Peptides. *Curr. Opin. Pharmacol.* **2019**, *47*, 8−13.

(9) Bottens, R. A.; Yamada, T. Cell-Penetrating Peptides (CPPs) as Therapeutic and Diagnostic Agents for Cancer. *Cancers* **2022**, *14* (22), 5546.

(10) Liu, H.; Tu, M.; Cheng, S.; Chen, H.; Wang, Z.; Du, M. An Anticoagulant Peptide from Beta-Casein: Identification, Structure and Molecular Mechanism. *Food Funct.* **2019**, *10* (2), 886−892.
(11) Agoni, C.; Stavropoulos, I.; Kirwan, A.; Mysior, M. M.; Holton, T.; Kranjc, T.; Simpson, J. C.; Roche, H. M.; Shields, D. C. Cell-Penetrating Milk-Derived Peptides with a Non-Inflammatory Profile. *Molecules* **2023**, *28* (19), 6999.
(12) Nhàn, N. T. T.; Yamada, T.; Yamada, K. H. Peptide-Based Agents for Cancer Treatment: Current Applications and Future Directions. *Int. J. Mol. Sci.* **2023**, *24* (16), 12931.
(13) Yamada, T.; Mehta, R. R.; Lekmine, F.; Christov, K.; King, M. L.; Majumdar, D.; Shilkaitis, A.; Green, A.; Bratescu, L.; Beattie, C. W.; Das Gupta, T. K. A Peptide Fragment of Azurin Induces a P53-Mediated Cell Cycle Arrest in Human Breast Cancer Cells. *Mol. Cancer Ther.* **2009**, *8* (10), 2947−2958.
(14) Lulla, R. R.; Goldman, S.; Yamada, T.; Beattie, C. W.; Bressler, L.; Pacini, M.; Pollack, I. F.; Fisher, P. G.; Packer, R. J.; Dunkel, I. J.; Dhall, G.; Wu, S.; Onar, A.; Boyett, J. M.; Fouladi, M. Phase I Trial of P28 (NSC745104), a Non-HDM2-Mediated Peptide Inhibitor of P53 Ubiquitination in Pediatric Patients with Recurrent or Progressive Central Nervous System Tumors: A Pediatric Brain Tumor Consortium Study. *Neuro-Oncology* **2016**, *18* (9), 1319−1325.
(15) Mander, S.; Gorman, G. S.; Coward, L. U.; Christov, K.; Green, A.; Das Gupta, T. K.; Yamada, T. The Brain-Penetrant Cell-Cycle Inhibitor P28 Sensitizes Brain Metastases to DNA-Damaging Agents. *Neurooncol. Adv.* **2023**, *5* (1), No. vdad042, DOI: 10.1093/noajnl/vdad042.
(16) Guidotti, G.; Brambilla, L.; Rossi, D. Cell-Penetrating Peptides: From Basic Research to Clinics. *Trends Pharmacol. Sci.* **2017**, *38* (4), 406−424.
(17) Lampi, K. J.; Ma, Z.; Shih, M.; Shearer, T. R.; Smith, J. B.; Smith, D. L.; David, L. L. Sequence Analysis of BA3, BB3, and BA4 Crystallins Completes the Identification of the Major Proteins in Young Human Lens. *J. Biol. Chem.* **1997**, *272* (4), 2268−2275.
(18) Bron, A. J.; Vrensen, G. F. J. M.; Koretz, J.; Maraini, G.; Harding, J. J. The Ageing Lens. *Ophthalmologica* **2000**, *214* (1), 86−104.
(19) Bloemendal, H.; de Jong, W.; Jaenicke, R.; Lubsen, N. H.; Slingsby, C.; Tardieu, A. Ageing and Vision: Structure, Stability and Function of Lens Crystallins. *Prog. Biophys. Mol. Biol.* **2004**, *86* (3), 407−485.
(20) Moreau, K. L.; King, J. A. Protein Misfolding and Aggregation in Cataract Disease and Prospects for Prevention. *Trends Mol. Med.* **2012**, *18* (5), 273−282.
(21) Lam, D.; Rao, S. K.; Ratra, V.; Liu, Y.; Mitchell, P.; King, J.; Tassignon, M.-J.; Jonas, J.; Pang, C. P.; Chang, D. F. Cataract. *Nat. Rev. Dis Primers* **2015**, *1* (1), No. 15014.
(22) Murthy, G.; Gupta, S.; John, N.; Vashist, P. Current Status of Cataract Blindness and Vision 2020: The Right to Sight Initiative in India. *Indian J. Ophthalmol* **2008**, *56* (6), 489.
(23) National Programme for Control of Blindness and Visual Impairment: State Wise Targets & Achievement for Various Eye Diseases during 2019−20. https://dghs.gov.in/WriteReadData/userfiles/file/NPCBVI/LOCAL_REF_4176_1620115567508.pdf.
(24) Parveen, S. *Films from the Cataractous Eye Protein Isolate: Preparation, Characterization and Applications*; Indian Institute of Technology Kharagpur: Kharagpur, 2020. http://www.idr.iitkgp.ac.in/xmlui/handle/123456789/9870.
(25) Parveen, S.; Chaudhury, S.; Dasgupta, S. Tuning the Mechanical and Physicochemical Properties of Cross-Linked Protein Films. *Biopolymers* **2019**, *110* (10), No. e23321, DOI: 10.1002/bip.23321.
(26) Parveen, S.; Ghosh, P.; Mitra, A.; Gupta, S.; Dasgupta, S. Preparation, Characterization, and in Vitro Release Study of Curcumin-Loaded Cataractous Eye Protein Isolate Films. *Emergent Mater.* **2019**, *2* (4), 475−486.
(27) Parveen, S.; Chaudhury, P.; Dasmahapatra, U.; Dasgupta, S. Biodegradable Protein Films from Gallic Acid and the Cataractous Eye Protein Isolate. *Int. J. Biol. Macromol.* **2019**, *139*, 12−20.
(28) Gasteiger, E.; Hoogland, C.; Gattiker, A.; Duvaud, S.; Wilkins, M. R.; Appel, R. D.; Bairoch, A. Protein Analysis Tools on the ExPASy Server 571 571 From: The Proteomics Protocols Handbook Protein Identification and Analysis Tools on the ExPASy Server.
(29) Dietrich, L.; Rathmer, B.; Ewan, K.; Bange, T.; Heinrichs, S.; Dale, T. C.; Schade, D.; Grossmann, T. N. Cell Permeable Stapled Peptide Inhibitor of Wnt Signaling That Targets β-Catenin Protein-Protein Interactions. *Cell Chem. Biol.* **2017**, *24* (8), 958−968.e5.
(30) LAMPI, K. J.; MA, Z.; HANSON, S. R. A.; AZUMA, M.; SHIH, M.; SHEARER, T. R.; SMITH, D. L.; SMITH, J. B.; DAVID, L. L. Age-Related Changes in Human Lens Crystallins Identified by Two-Dimensional Electrophoresis and Mass Spectrometry. *Exp. Eye Res.* **1998**, *67* (1), 31−43.
(31) Chaudhury, S.; Ghosh, I.; Saha, G.; Dasgupta, S. EGCG Prevents Tryptophan Oxidation of Cataractous Ocular Lens Human γ-Crystallin in Presence of H2O2. *Int. J. Biol. Macromol.* **2015**, *77*, 287−292.
(32) Chowdhury, P.; Parveen, S.; Sarker, R.; Dasgupta, S. Enhancing the Properties of Films Prepared from the Cataractous Eye Protein Isolate (CEPI) for Potential Biomedical Applications. *Emergent Mater.* **2022**, *5* (3), 621−629.
(33) Kyte, J.; Doolittle, R. F. A Simple Method for Displaying the Hydropathic Character of a Protein. *J. Mol. Biol.* **1982**, *157* (1), 105−132.
(34) Yu, C.; Zheng, L.; Cai, Y.; Zhao, Q.; Zhao, M. Desirable Characteristics of Casein Peptides with Simultaneously Enhanced Emulsion Forming Ability and Antioxidative Capacity in O/W Emulsion. *Food Hydrocoll.* **2022**, *131*, No. 107812, DOI: 10.1016/j.foodhyd.2022.107812.
(35) Gomez, J. A.; Chen, J.; Ngo, J.; Hajkova, D.; Yeh, I.-J.; Gama, V.; Miyagi, M.; Matsuyama, S. Cell-Penetrating Penta-Peptides (CPP5s): Measurement of Cell Entry and Protein-Transduction Activity. *Pharmaceuticals* **2010**, *3* (12), 3594−3613.
(36) Rhee, M.; Davis, P. Mechanism of Uptake of C105Y, a Novel Cell-Penetrating Peptide. *J. Biol. Chem.* **2006**, *281* (2), 1233−1240.
(37) Hou, K. K.; Pan, H.; Lanza, G. M.; Wickline, S. A. Melittin Derived Peptides for Nanoparticle Based SiRNA Transfection. *Biomaterials* **2013**, *34* (12), 3110−3119.
(38) Galdiero, S.; Falanga, A.; Morelli, G.; Galdiero, M. GH625: A Milestone in Understanding the Many Roles of Membranotropic Peptides. *Biochim. Biophys. Acta, Biomembr.* **2015**, *1848* (1), 16−25.
(39) Baoum, A.; Ovcharenko, D.; Berkland, C. Calcium Condensed Cell Penetrating Peptide Complexes Offer Highly Efficient, Low Toxicity Gene Silencing. *Int. J. Pharm.* **2012**, *427* (1), 134−142.
(40) Chu, D.; Xu, W.; Pan, R.; Ding, Y.; Sui, W.; Chen, P. Rational Modification of Oligoarginine for Highly Efficient SiRNA Delivery: Structure−Activity Relationship and Mechanism of Intracellular Trafficking of SiRNA. *Nanomedicine* **2015**, *11* (2), 435−446.
(41) de Coupade, C.; Fittipaldi, A.; Chagnas, V.; Michel, M.; Carlier, S.; Tasciotti, E.; Darmon, A.; Ravel, D.; Kearsey, J.; Giacca, M.; Cailler, F. Novel Human-Derived Cell-Penetrating Peptides for Specific Subcellular Delivery of Therapeutic Biomolecules. *Biochem. J.* **2005**, *390* (2), 407−418.
(42) Nielsen, E. J. B.; Yoshida, S.; Kamei, N.; Iwamae, R.; Khafagy, E.-S.; Olsen, J.; Rahbek, U. L.; Pedersen, B. L.; Takayama, K.; Takeda-Morishita, M. In Vivo Proof of Concept of Oral Insulin Delivery Based on a Co-Administration Strategy with the Cell-Penetrating Peptide Penetratin. *J. Controlled Release* **2014**, *189*, 19−24.
(43) Futaki, S.; Suzuki, T.; Ohashi, W.; Yagami, T.; Tanaka, S.; Ueda, K.; Sugiura, Y. Arginine-Rich Peptides. *J. Biol. Chem.* **2001**, *276* (8), 5836−5840.
(44) Eggimann, G. A.; Blattes, E.; Buschor, S.; Biswas, R.; Kammer, S. M.; Darbre, T.; Reymond, J.-L. Designed Cell Penetrating Peptide Dendrimers Efficiently Internalize Cargo into Cells. *Chem. Commun.* **2014**, *50* (55), 7254−7257.
(45) Johansson, H. J.; El-Andaloussi, S.; Holm, T.; Mäe, M.; Jänes, J.; Maimets, T.; Langel, Ü. Characterization of a Novel Cytotoxic Cell-penetrating Peptide Derived From P14ARF Protein. *Mol. Ther.* **2008**, *16* (1), 115−123.

https://doi.org/10.1021/acsomega.3c07665
ACS Omega 2024, 9, 14840−14848

(46) Simeoni, F. Insight into the Mechanism of the Peptide-Based Gene Delivery System MPG: Implications for Delivery of SiRNA into Mammalian Cells. *Nucleic Acids Res.* **2003**, *31* (11), 2717−2724.
(47) Wada, S.-i.; Hashimoto, Y.; Kawai, Y.; Miyata, K.; Tsuda, H.; Nakagawa, O.; Urata, H. Effect of Ala Replacement with Aib in Amphipathic Cell-Penetrating Peptide on Oligonucleotide Delivery into Cells. *Bioorg. Med. Chem.* **2013**, *21* (24), 7669−7673.
(48) Pae, J.; Säälik, P.; Liivamägi, L.; Lubenets, D.; Arukuusk, P.; Langel, Ü.; Pooga, M. Translocation of Cell-Penetrating Peptides across the Plasma Membrane Is Controlled by Cholesterol and Microenvironment Created by Membranous Proteins. *J. Controlled Release* **2014**, *192*, 103−113.
(49) Amin, M. O.; D'Cruz, B.; Madkour, M.; Al-Hetlani, E. Magnetic Nanocomposite-Based SELDI Probe for Extraction and Detection of Drugs, Amino Acids and Fatty Acids. *Microchim. Acta* **2019**, *186* (8), No. 503, DOI: 10.1007/s00604-019-3623-2.
(50) Yoshida, T.; Tomioka, I.; Nagahara, T.; Holyst, T.; Sawada, M.; Hayes, P.; Gama, V.; Okuno, M.; Chen, Y.; Abe, Y.; Kanouchi, T.; Sasada, H.; Wang, D.; Yokota, T.; Sato, E.; Matsuyama, S. Bax-Inhibiting Peptide Derived from Mouse and Rat Ku70. *Biochem. Biophys. Res. Commun.* **2004**, *321* (4), 961−966.
(51) Rashidi, L.; Ganji, F.; Vasheghani-Farahani, E. Fluorescein Isothiocyanate-dyed Mesoporous Silica Nanoparticles for Tracking Antioxidant Delivery. *IET Nanobiotechnol.* **2017**, *11* (4), 454−462.
(52) Richard, J. P.; Melikov, K.; Vives, E.; Ramos, C.; Verbeure, B.; Gait, M. J.; Chernomordik, L. V.; Lebleu, B. Cell-Penetrating Peptides. *J. Biol. Chem.* **2003**, *278* (1), 585−590.

https://doi.org/10.1021/acsomega.3c07665
ACS Omega 2024, 9, 14840−14848